Bioresource Technology 169 (2014) 220–228

Contents lists available at ScienceDirect

Bioresource Technology

journal homepage: www.elsevier.com/locate/biortech

# Synergistic effect on thermal behavior during co-pyrolysis of lignocellulosic biomass model components blend with bituminous coal

Zhiqiang Wu, Shuzhong Wang *, Jun Zhao, Lin Chen, Haiyu Meng

*Key Laboratory of Thermo-Fluid Science and Engineering, Ministry of Education, School of Energy and Power Engineering, Xi'an Jiaotong University, Xi'an, Shaanxi 710049, PR China*

## HIGHLIGHTS

- Co-pyrolysis behavior of lignocellulosic biomass components and bituminous coal was explored.
- Positive and/or negative synergistic effects were observed during co-pyrolysis of the mixtures.
- Kinetic parameter was solved via using model-free method (Kissinger–Akahira–Sunose).
- Nonadditivity performance on the activation energy values of the mixtures was observed.

## ARTICLE INFO

*Article history:*
Received 19 May 2014
Received in revised form 27 June 2014
Accepted 28 June 2014
Available online 5 July 2014

*Keywords:*
Synergistic effect
Lignocellulosic biomass
Co-pyrolysis
Kinetics
Coal

## ABSTRACT

Co-thermochemical conversion of lignocellulosic biomass and coal has been investigated as an effective way to reduce the carbon footprint. Successful evaluating on thermal behavior of the co-pyrolysis is prerequisite for predicting performance and optimizing efficiency of this process. In this paper, pyrolysis and kinetics characteristics of three kinds of lignocellulosic biomass model components (cellulose, hemicellulose, and lignin) blended with a kind of Chinese bituminous coal were explored by thermogravimetric analyzer and Kissinger–Akahira–Sunose method. The results indicated that the addition of model compounds had different synergistic effects on thermal behavior of the bituminous coal. The cellulose showed positive synergistic effects on the thermal decomposition of the coal bituminous coal with lower char yield than calculated value. For hemicellulose and lignin, whether positive or negative synergistic was related to the mixed ratio and temperature range. The distribution of the average activation energy values for the mixtures showed nonadditivity performance.



## 1. Introduction

Lignocellulosic biomass has attracted extensive attention worldwide as a promising renewable and $CO_2$ neutral energy source, which also provides approximately 14% of the world's energy supply (Lopez-Gonzalez et al., 2013; Sanchez-Silva et al., 2012; Zhang et al., 2011). Thermochemical conversion of lignocellulosic biomass is one of the most promising processes for its wide adaptability of feedstock and diversification of products (Guo et al., 2014; Maschio et al., 1992; Shen et al., 2010). Nevertheless, widespread applications for thermochemical conversion of lignocellulosic biomass in energy supplying is limited due to the seasonal availability, extensive distribution and heterogeneity of the biomass (Parshetti et al., 2013; Wu et al., 2014).

Co-thermochemical conversion of lignocellulosic biomass and coal can overcome these obstacles and utilize coal in an environmentally friendly way (Habibi et al., 2013; Weiland et al., 2012). As a precursor for co-combustion and co-gasification, co-pyrolysis have significant influence on the kinetic characteristic and products distribution of the further process. Co-pyrolysis is not only a promising co-thermochemical conversion technology for producing varieties of fuels and chemical compounds, but also a key step of co-combustion and co-gasification (Sanchez-Silva et al., 2012; Xu and Chen, 2013). Information about the pyrolytic characteristics and kinetic analysis during the co-pyrolysis process is very necessary for design and operation of co-thermochemical conversion. Furthermore, a knowledge about the pyrolytic characteristics and kinetics during co-pyrolysis process has a great importance for product yield control and performance promotion.

As a prerequisite for product yield control and performance improve of the co-pyrolysis process, much attention has been devoted on the on the pyrolytic characteristics and kinetic analysis

* Corresponding author. Tel.: +86 29 82665157; fax: +86 29 82668708.
*E-mail address:* szwang@aliyun.com (S. Wang).

http://dx.doi.org/10.1016/j.biortech.2014.06.105
0960-8524/

of different rank coals blend with a variety of lignocellulosic biomass, including rice straw (Yuan et al., 2012), switch grass (Weiland et al., 2012), hazelnut shell (Haykiri-Acma and Yaman, 2010), corn and sugarcane residues (Aboyade et al., 2013) from agricultural residues, pine sawdust (Soncini et al., 2013) and pine chips (Pan et al., 1996) from forestry residues. However, due to the wide varieties and heterogeneity of the lignocellulosic biomass, different conclusions on the pyrolytic characteristics and kinetic analysis were obtained. Several researchers have found that higher volatile yields were produced than the values calculated from individual fuels, which can be called synergistic effects (Chen et al., 2012; Haykiri-Acma and Yaman, 2010; Kar, 2011; Onay et al., 2007; Park et al., 2010; Vamvuka and Sfakiotakis, 2011; Wu et al., 2014). While some researchers disagreed with the existence of synergy effect during co-pyrolysis (Moghtaderi et al., 2004; Pan et al., 1996). Furthermore, the main components of lignocellulosic biomass are cellulose, hemicellulose and lignin (Shen et al., 2010; Zhang et al., 2011). The pyrolytic and kinetic behavior of individual components in biomass blend with coal during co-pyrolysis process is great important for gaining insight into the mechanism of co-pyrolysis. However, to our best of knowledge, there is no report on thermal behavior during co-pyrolysis of lignocellulosic biomass individual components and coal. For a better understanding of co-pyrolysis process and design of efficient co-thermochemical plants, there is an unmet need to study thermal behavior during co-pyrolysis of biomass individual components and coal.

The aim of this paper is to investigate the thermal behavior of lignocellulosic biomass individual model compounds and bituminous coal during co-pyrolysis for gaining a deep knowledge of the co-thermochemical conversion. Pyrolytic behavior of the lignocellulosic biomass model compounds (cellulose, hemicellulose and lignin) and bituminous coal mixtures were investigated via a thermogravimetric analyzer under an inert atmosphere. The kinetics parameters were obtained using by non-isothermal thermogravimetric analysis. This paper provides a further understanding of the interaction between coal and lignocellulosic biomass on molecular level.

## 2. Methods

### 2.1. Materials

The main model components of lignocellulosic biomass were purchased from Sigma–Aldrich Co., Ltd, including cellulose (CE, CAS number: 9004-34-6), hemicellulose (HCE, CAS number: 9014-63-5) and lignin (LIG, CAS number: 8068-05-1). The bituminous coal (BC) was collect from north of Shaanxi, China. The model components were screened individually and collected the particle size less than 74 μm for experiment. The bituminous coal was grinded into less than 74 μm and mixed with the model components well. The proximate and ultimate analyses of the raw samples were shown in Table 1. The mixture samples of coal and cellulose were named as "BCCE3-1", "BCCE1-1" and "BCCE1-3", which the mass ratio of cellulose was 25%, 50% and 75%. The mixture samples of coal and hemicellulose/lignin were named as the same way.

### 2.2. Experimental apparatus and methods

Thermogravimetric (TG) and derivative thermogravimetric (DTG) experiments of the raw and mixture samples were carried out through a WCT-2C TGA manufactured by Beijing Optical Instrument Factory. In each experiment, about 10 mg of the sample was used to mitigate the effect of heat and mass transfer. The experiments were performed from room temperature to 950 °C at the heating rates of 10, 20, 40 °C $min^{-1}$ under high purity nitrogen with 60 ml $min^{-1}$. In order to quantify the performance of volatile matters releasing, he devolatilization index ($D_i$) (Jianguo and Zhaolong, 1999; Wu et al., 2014) was defined:

$$D_i = R_{max}/(T_{in}T_{max}\Delta T_{1/2}) \quad (1)$$

where $R_{max}$ is the maximum decomposition rate, $T_{in}$ is the initial devolatilization temperature, $T_{max}$ is the maximum mass loss temperature. $T_{in}$ and $T_{max}$ can be obtained from the TG and DTG curves (Yan and Chen, 2007). $\Delta T_{1/2}$ is the temperature interval when $R_d/R_{max}$ equals 1/2. $R_d$ is the decomposition rate, $R_d = -dm_t/dt$, where $m_t$ is the mass of the raw sample at time $t$. $R_{max}$ and $R_d$ can be obtained from the DTG curves.

In addition, the synergistic effect during co-pyrolysis process of the three model compounds and bituminous coal can be estimated from the deviation of the experimental and calculated values of the TG curves (Park et al., 2010). The $\Delta W$ was defined to evaluate the degree of the synergistic effects:

$$\Delta W = W_{Experimental} - W_{Calculated} \quad (2)$$

where $\Delta W$ is the relative mass loss deviation (%), which represents the degree of synergistic effects. $W_{Experimental}$ is the experimental value from the TG curve of the mixture samples. $W_{Calculated}$ is calculated as the sum of the TG curves of each individual sample, which can be obtained by:

$$W_{Calculated} = X_M W_M + X_B W_B \quad (3)$$

where $X_M$ and $X_B$ are the mass fraction of the model component and coal in the mixture samples, and $W_M$ and $W_B$ are the weight losses from the TG curves of model component and coal under the same condition of the mixture individually.

**Table 1**
Proximate and ultimate analyses of the raw samples.

| | BC | CE | HCE | LIG |
|---|---|---|---|---|
| *Proximate analysis* (*wt.%, ad*) | | | | |
| Moisture, M | 4.18 | 4.67 | 5.76 | 3.38 |
| Ash, A | 15.38 | 0.07 | 3.61 | 3.62 |
| Volatile, V | 30.56 | 93.37 | 77.71 | 60.35 |
| Fixed carbon, FC | 49.88 | 1.89 | 12.92 | 32.65 |
| *Ultimate analysis* (*wt.%, daf*) | | | | |
| Carbon, C | 79.31 | 51.47 | 40.18 | 61.35 |
| Hydrogen, H | 4.72 | 2.87 | 5.53 | 5.05 |
| Nitrogen, N | 1.03 | 1.69 | 2.71 | 1.13 |
| Sulfur, $S^t$ | 1.3 | 0.03 | – | 0.69 |
| Oxygen, $O^c$ | 13.38 | 43.93 | 51.58 | 31.78 |
| High-heating value (MJ $kg^{-1}$, ad) | 25.44 | 16.71 | 15.21 | 17.98 |

ad: air-dried; daf: dry ash-free; t: total content; c: calculated by difference.

### 2.3. Kinetic method

As we all known that from the iso-conversional method, the value of activation energy ($E$) can be obtained easily without considering the reaction mechanism (Wu et al., 2014; Xu and Chen, 2013). The Kissinger–Akahira–Sunose (KAS) (Kissinger, 1957) method was introduced to solve the activation energy for their higher relatively. The KAS method were expressed as:

$$\ln(\beta/T_\alpha^2) = \ln[AR/EG(\alpha)] - E/ET_\alpha \quad (4)$$

where $\beta$ is the heating rate (°C $min^{-1}$), $\alpha = (m_0 - m_t)/(m_0 - m_\infty)$ and $\alpha$ is the conversion degree of the raw sample, where $t$ is time, $m_0$ is and $m_\infty$ are the initial mass and final mass of the raw sample, respectively. $m_t$ is the mass of the raw sample at time $t$. $A$ and $E$ are the pre-exponential factor and activation energy (kJ $mol^{-1}$), $R$ is the universal gas constant (kJ $mol^{-1}$ $K^{-1}$), $T_\alpha$ is the temperature of the sample with a raw sample under conversion degree of $\alpha$

(K), and $G(\alpha)$ is the integration function of the reaction model. The value of $\ln(\beta/T_\alpha^2)$ and $\ln\beta$ versus $1/T$ under constant $\alpha$ at several $\beta$ can be obtained by linear regression, and then the $E$ at various $\alpha$ could be determined respectively.

## 3. Results and discussion

### 3.1. Pyrolysis characteristics

#### 3.1.1. Individual samples

Fig. 1 shows the TG and DTG curves of the bituminous coal (BC), cellulose (CE), hemicellulose (HCE) and lignin (LIG) under nitrogen at the heating rate of 20 °C min$^{-1}$. It can be seen from Fig. 1, the evolutions of the TG and DTG curves of the raw samples were different from each other. The pyrolytic process of the BC, CE and LIG showed one stage without considering the evaporation of moisture. The decomposition of the BC began around 370 °C and suffer a continuous mass loss. For CE, an obvious mass loss stage was observed from 300 to 410 °C in a narrow temperature range, in which the CE decomposed rapidly with consuming products releasing. The decomposition of LIG was prior to the BC, which began around 200 °C and had a continuous mass loss over a temperature range of 200–900 °C. The Pyrolysis temperature range of those model compounds were agree with the results of other researchers (Pottmaier et al., 2013; Sanchez-Silva et al., 2012; Shen et al., 2010). On the other hand, the pyrolytic process of the HCE showed two distinct peaks with steady mass loss from 195 to 400 °C. The first peak is related to the cracking of side units and the second one is ascribed to the decomposition of the main chain (Dumitriu, 2012; Lopez-Gonzalez et al., 2013).

Several characteristic parameters about pyrolysis process of the BC and model compounds under $\beta$ of 20 °C min$^{-1}$ were listed in Table 2. The DTG curve peak values of BC and LIG were lower than those of CE and HCE. The BC's and LIG's DTG curves were observed with the intensities of 1.39 mg min$^{-1}$ and 1.26 mg min$^{-1}$, at 461 °C and 368 °C, respectively. CE's DTG curve have the maximum peak value at 355 °C with 11.66 mg min$^{-1}$. The intensity of the HCE's DTG curve first peak was 6.03 mg min$^{-1}$ at 258 °C, then increased to 7.07 mg min$^{-1}$ at 299 °C. Furthermore, the performance of volatile matters release was evaluated by the devolatilization index ($D_i$). As can be found from Eq. (1)that the higher $D_i$ indicated an easier releasing of the volatile. The $D_i$ of the BC and model compounds were listed in Table 2. Table 2 showed that $D_i$ of the coal was 4.97, which agreed with the results of our previous research and other researchers (Jianguo and Zhaolong, 1999; Wang et al., 2011; Wu et al., 2014). While $D_i$ of the CE, HCE and LIG were 246.49, 141.36 and 10.77, respectively. Whether the addition of model compounds will promote the performance of volatile matters release of BC or not was discussed in Section 3.1.2.

#### 3.1.2. Mixed samples

The pyrolysis characteristics of BC blended with CE, HCE and LIG were shown in Figs. 2–4 respectively. Pyrolysis characteristic parameters of the mixed samples under $\beta$ of 20 °C min$^{-1}$ were also listed in Table 2. Fig. 2 shows the TG and DTG curves of BC, CE and their mixtures under 20 °C min$^{-1}$. With the mass ratio of CE increased, the mass of residual char at 950 °C decreased gradually. Addition of the CE into coal with a mass ratio of 25% (BCCE3-1) and 50% (BCCE1-1) made the intensity of the first peak increase to 5.45 mg min$^{-1}$ at 346 °C and 10.02 mg min$^{-1}$ at 348 °C. The intensity of the second peak of BCCE3-1 and BCCE1-1 were lower than that of BC, with 1.33 mg min$^{-1}$ at 467 °C and 0.69 mg min$^{-1}$ at 450 °C, respectively. When the proportion of the CE reached 75%, the intensity of the peak increased to the maximum value among the five samples, with 14.32 mg min$^{-1}$ at 349 °C. The highest intensity peak of BCCE1-3 may be related to the interaction of the CE and BC. Table 2 showed that $D_i$ of the BC and CE mixed samples increased from 97.12 to 260.62 with the increasing mass ratio of CE. This indicated that the performance of the mixture volatile releasing was promoted by the adding of CE.

Pyrolysis characteristics of the BC, HCE and their mixtures were illustrated in Fig. 3. It can be seen from Fig. 3, the final residual char decreased with the rise of HCE mass ratio, which were similar to those of BC and CE mixed samples. The DTG curves of BC and HCE mixed samples and HCE showed vivid evident peaks between 50 and 150 °C due to the release of moisture from depolymerization of HCE. For HCE the rate of degradation was the largest with two distinct peaks between 195 and 400 °C. The rate for BC and HCE mixed samples were between those of BC and HCE. Data in Table 2 shows that the intensity of the first peak were 1.34 mg min$^{-1}$ at 293 °C, 3.37 mg min$^{-1}$ at 296 °C and 5.37 mg min$^{-1}$ at 298 °C for BCHCE3-1, BCHCE1-1 and BCHCE1-3, respectively. The values of the second peak were decreased from 0.84 mg min$^{-1}$ at 464 °C to 0.74 mg min$^{-1}$ at 476 °C. The first peak was ascribed to the decomposition of HCE and the second peak was related to the decomposition of BC. Compared to pure BC, the degradation temperature of BC in BC and HCE mixtures was reduced to 464–476 °C with the intensity was also reduced. This suggests the synergetic effect between the BC and HCE may exist. The $D_i$ of the BC and HCE mixed samples increased from 23.64 to 85.16 with the increasing mass ratio of HCE. While the $D_i$ of pure HCE was 141.36, thirty times more than that of BC.

Observed thermal behavior of BC, LIG and their mixtures during co-pyrolysis at a heating rate of 20 °C min$^{-1}$ is shown in Fig. 4. The mass of residual char decreased with increasing LIG content, which

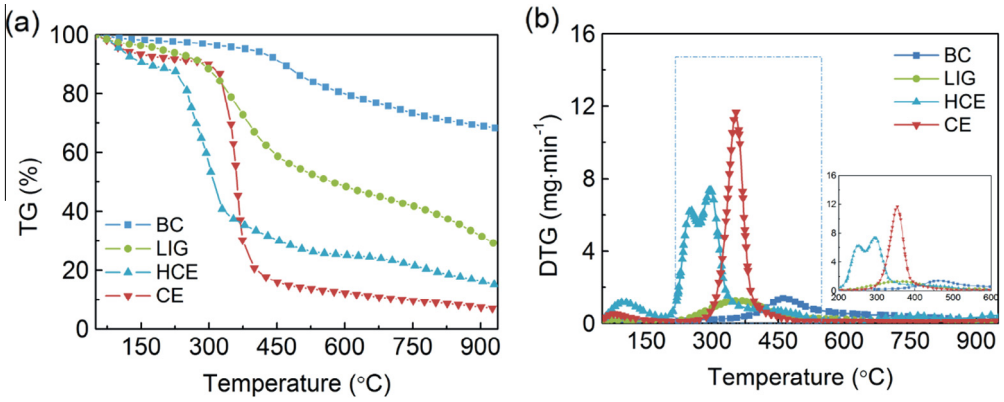


**Fig. 1.** Pyrolysis characteristics of the bituminous coal (BC), cellulose (CE), hemicellulose (HCE) and lignin (LIG) in TGA with $\beta$ = 20 °C min$^{-1}$, (a) TG curves, (b) DTG curves.

**Table 2**
Pyrolysis parameters of the BC, CE and their mixtures with $\beta = 20\ ^{\circ}C\ min^{-1}$.

| Parameters | | BC | 25% CE | 50% CE | 75% CE | CE | 25% HCE | 50% HCE | 75% HCE | HCE | 25% LIG | 50% LIG | 75% LIG | LIG |
|---|---|---|---|---|---|---|---|---|---|---|---|---|---|---|
| $T_{in}$ (°C) | Initial devolatilization temperature | 370 | 318 | 327 | 328 | 325 | 208 | 201 | 230 | 200 | 271 | 274 | 275 | 200 |
| $T_1$ (°C) | Temperature of the first DTG peak | 461 | 346 | 348 | 349 | 355 | 293 | 296 | 298 | 258 | 349 | 348 | 371 | 368 |
| $R_1$ (mg min$^{-1}$) | Decomposition rate of the first DTG peak | 1.39 | 5.45 | 10.02 | 14.32 | 11.66 | 1.34 | 3.37 | 5.37 | 6.03 | 0.74 | 1.46 | 2.17 | 1.26 |
| $T_2$ (°C) | Temperatures of the second DTG peak | – | 467 | 450 | – | – | 464 | 468 | 476 | 299 | 461 | – | – | – |
| $R_2$ (mg min$^{-1}$) | Decomposition rate of the second DTG peak | – | 1.33 | 0.69 | – | – | 0.84 | 0.83 | 0.74 | 7.27 | 0.88 | – | – | – |
| $R_{max}$ (mg min$^{-1}$) | Maximum decomposition rate | 1.39 | 5.45 | 10.02 | 14.32 | 11.66 | 1.34 | 3.37 | 5.37 | 7.27 | 0.88 | 1.46 | 2.17 | 1.26 |
| $T_{max}$ (°C) | Temperature of maximum decomposition rate | 461 | 346 | 348 | 349 | 355 | 293 | 296 | 298 | 299 | 461 | 348 | 371 | 368 |
| $\Delta T_{1/2}$ (°C) | Temperature interval when $R_d/R_{max} = 1/2$ | 164 | 51 | 53 | 48 | 41 | 93 | 94 | 92 | 86 | 378 | 234 | 165 | 159 |
| $D_i$ ($10^{-8}$mg min$^{-1}$ °C$^{-3}$) | Devolatilization index of the sample | 4.97 | 97.12 | 166.14 | 260.62 | 246.49 | 23.64 | 60.26 | 85.16 | 141.36 | 1.86 | 6.54 | 12.89 | 10.77 |

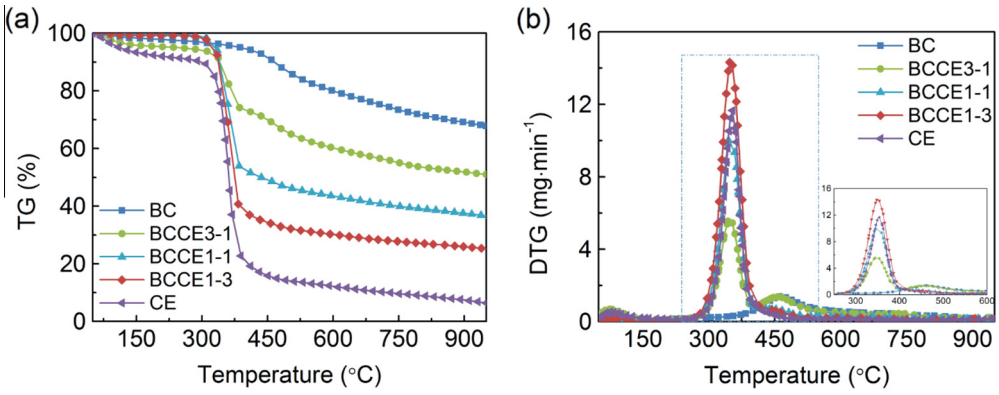


**Fig. 2.** Pyrolysis characteristics of the bituminous coal (BC), cellulose (CE) and their mixtures under various mass ratios in TGA with $\beta = 20\ ^{\circ}C\ min^{-1}$, (a) TG curves, (b) DTG curves.

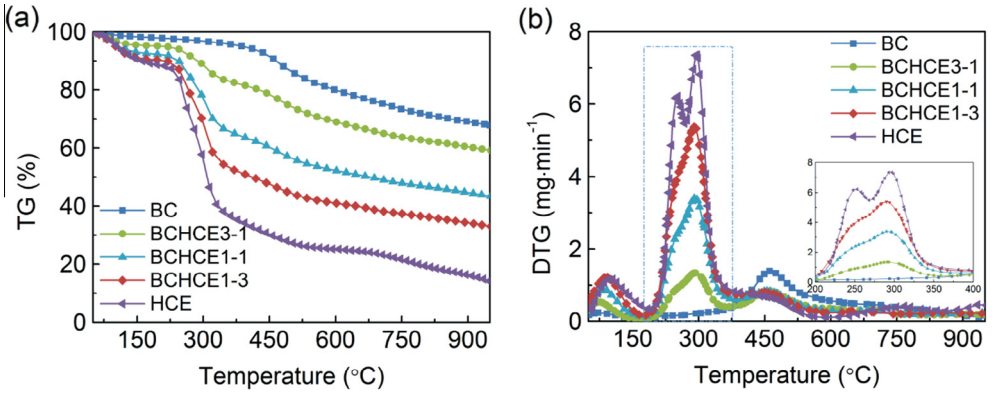


**Fig. 3.** Pyrolysis characteristics of the bituminous coal (BC), hemicellulose (HCE) and their mixtures under various mass ratios in TGA with $\beta = 20\ ^{\circ}C\ min^{-1}$, (a) TG curves, (b) DTG curves.

was due to the high volatile content in LIG samples compared to the BC. Compared to BCCE mixed samples and BCHCE mixed samples, the tendency of BCLIG mixtures were not very regular. For BC, LIG and BCLIG1-3, there was a single peak for devolatilization without taking into account evaporation of moisture. Two relatively obvious peaks were observed for BCLIG3-1, with 0.74 mg min$^{-1}$ at 349 °C and 0.88 at 461 °C. The DTG curves of BCLIG1-1 showed a primary peak with a slight depression. As can

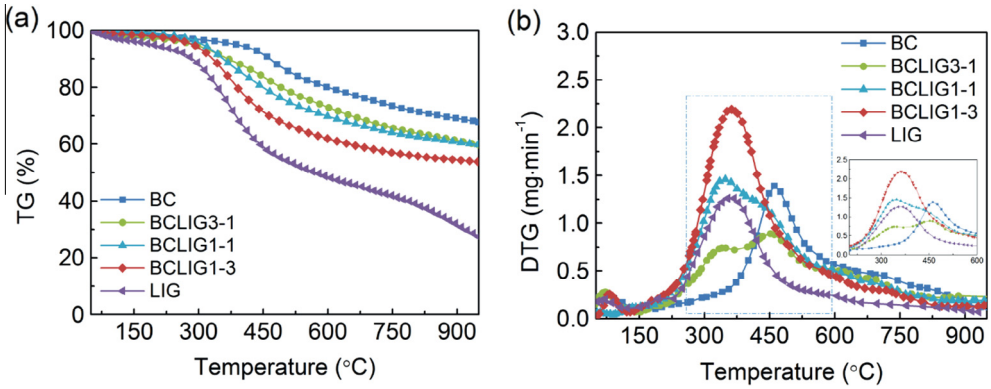


**Fig. 4.** Pyrolysis characteristics of the bituminous coal (BC), lignin (LIG), and their mixtures under various mass ratios in TGA with $\beta$ = 20 °C min$^{-1}$, (a) TG curves, (b) DTG curves.

be seen in Table 2, with the increment of the LIG mass ratio, the number of the peak decreased from two to one and the intensity increased from 0.74 mg min$^{-1}$ to 2.17 mg min$^{-1}$. Which indicated that the in interaction between BC and LIG did exist, resulting in the inhibition of BC devolatilization and the promotion of LIG devolatilization.

From the observations discussed above, it can be observed that the addition of the CE, HCE and LIG had different influence on the pyrolytic behavior of BC. The change in morphology and intensity of DTG curves and the variation tendency of $D_i$ indicated some hints of interaction between BC and model compounds. These phenomena indicated that the interaction between BC and model compounds cannot be ignored. The interaction effects will be discussed in Section 3.2.

### 3.2. Interaction effects between the BC and model compounds

The comparison of residual mass ratio from experimental TG curves of mixed samples to that calculated from weighted average of individual TG curves of BC and model compound were shown in Fig. 5. Fig. 5a and b present the variation trends of $W_{Experimental}$ and $W_{Calculated}$ with various CE ratios when $\beta$ equals 20 °C min$^{-1}$. For BCCE3-1, the value of $W_{Experimental}$ was lower than that of the $W_{Calculated}$ in the temperature range of experiment, indicating that the synergistic effect between BC and CE may exist, and this effect promoted the thermal decomposition of BC for higher volatiles. When the mass ratio of CE increased to 50% and 75%, the variation trends of $W_{Experimental}$ and $W_{Calculated}$ were different from that of 25% CE to a certain extent. The value of $W_{Experimental}$ was greater than that of the $W_{Calculated}$ over the temperature range of ambient temperature to 360 °C. While the temperature higher than 360 °C, the variation trends were in contrast with the previous temperature interval. In this study, the primary structure of cellulose was a polysaccharide composed of glucopyranose residues linked by β-1,4-glycosidic bonds with two kinds of end groups (reducing and non-reducing end groups) (Matsuoka et al., 2014; Moghtaderi et al., 2004). Thermal decomposition of CE primarily transformed into laevoglucose with the breakdown of glycosidic bonds, which can provide hydrogenous donor for BC pyrolysis (Richards, 1987). The volatile content in CE was nearly three times more than that of BC. As discussed in Section 3.1.1, the decomposition of CE was mainly happen in 300–410 °C. With the mass ratio of the CE increased, a large quantity volatile released in a relatively short time. Part of the volatile may stay in the gap between BC and CE particle and gather on the BC surface, which may also hinder the releasing of volatile from BC. Thus value of $W_{Experimental}$ was greater than that of the $W_{Calculated}$. However, with the rising of the temperature, the inner pressure of the BC and CE particles increased and the residues of the CE may flow, which was beneficial to the diffusion of volatile. Especially for the BCCE1-1, the minimum value of the $\Delta W$ was −10.79% at 400 °C. The root mean square (RMS) values of the deviation between the experimental value and calculated ($\Delta W$) were used to measure the synergistic effects in previous research (Sadhukhan et al., 2008). In this study, the RMS of the $\Delta W$ were 1.163, 4.686 and 1.858 for BCCE3-1, BCCE1-1 and BCCE1-3, which were ten times than those of reported in previous research (Sadhukhan et al., 2008; Yangali et al., 2014). These values indicated that there were synergistic effects between the BC and CE. The addition of CE to BC accelerated the decomposition of BC when temperature higher than 360 °C, resulted in less residual char.

The variation trends of $W_{Experimental}$ and $W_{Calculated}$ with various HCE ratios under $\beta$ equals 20 °C min$^{-1}$ were shown in Fig. 5c and d. It illustrated that all the deviation curves of the $W_{Experimental}$ and $W_{Calculated}$ values showed a slight decrease at temperature between ambient temperature and 150 °C and then kept an increasing tendency until the final pyrolysis temperature. The RMS values of the $\Delta W$ for BC and HCE blends varied between 1.112 and 1.869. This suggested that the synergistic effects existed between the BC and HCE during co-pyrolysis. However, the synergistic effects between BC and HCE were different from those between BC and CE. The adding of HCE to BC hindered the decomposition of BC under 25% and 75% HCE mass ratio over the temperature range of 200–950 °C, which can be called passive synergistic effect. For 50% HCE mass ratio, the blocking effect on the production of volatile during co-pyrolysis was less obvious than others.

As can be seen from Fig. 5e and f, the residual char yield of BC-LIG mixed samples calculated from the weighted averages of individual TG curves of BC and LIG showed obvious deviation from experimental TG data of mixed samples with different LIG ratios. The values of residual char fraction were even overlap, which may be due to the interaction between BC and LIG. The RMS values of $\Delta W$ were 2.528, 2.603 and 3.520 for BCLIG3-1, BCLIG1-1 and BCLIG1-3. This confirmed that there existed synergistic effects during co-pyrolysis of BC and LIG. Although the RSM value of BCLIG3-1 did not appear to be much different from that of BCLIG1-1, the effects on the residual char yield were different. When the mass ratio of LIG was 25%, the $W_{Experimental}$ was lower than the $W_{Calculated}$ at the whole temperature range, indicating the thermal decomposition was accelerated and produced less residual char. With the LIG mass ratio increased from 50% to 75%, the value of $W_{Experimental}$ was greater than that of $W_{Calculated}$, and the deviation ($\Delta W$) were increased with the pyrolysis temperature rising. The main component of LIG is heterogeneous aromatic polymer (Guo et al., 2014), and during the pyrolysis of pure LIG, the swelling of the LIG was observed. As the ratio of the LIG was lower in the BC-LIG blends

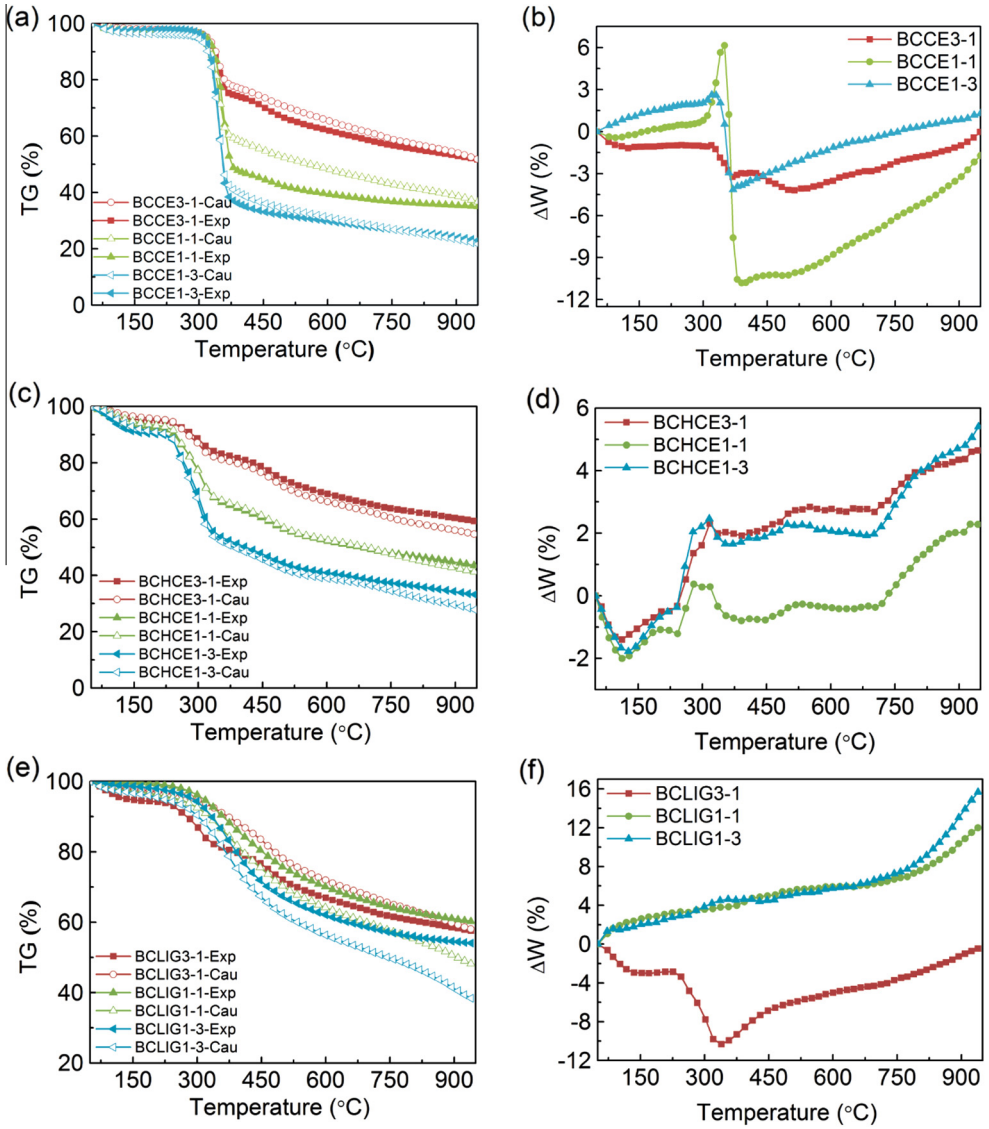


**Fig. 5.** TG curves comparison between the experimental and calculated value from the mixtures under 20 °C $min^{-1}$, (a) BC, CE and their mixtures, (b) $\Delta W$ for BC blended with CE, (c) BC, HCE and their mixtures, (d) $\Delta W$ versus for BC blended with HCE, (e) BC, LIG and their mixtures, (f) $\Delta W$ for BC blended with LIG.

(25% mass ratio in this paper), the swelling of LIG may provide micro-channel for the releasing of volatile. Furthermore, with the promotion of the LIG increasing from 50% to 75%, the degree of the swelling was aggravated, which could affect the transfer of volatile out of the particles. Thus part of the molecules and radicals residues may transform into carbonaceous through several polymerization and condensation reactions and deposited on the pores and gap of BC and LIG particles.

Remarkable synergy was found in the char yields during co-pyrolysis of BC blended with lignocellulosic biomass model components. As can be seen from Fig. 5, the three model components of lignocellulosic biomass had different influence on the co-pyrolysis process. Even the same model compound, different mixing ratios also showed various effects on the co-pyrolysis process. The formation of char was favored for BCHCE3-1 and BCHCE1-3 when temperature was higher than 200 °C, and the generation of volatile material was more inhibited when BCLIG1-1 and BCLIG1-3 decomposed from room temperature to 950 °C. For pyrolysis of BCCE3-1 and BCLIG3-1, more volatile material were generated.

Previous researchers reported the similar synergistic effect on char yields during co-pyrolysis of the coal blended with various lignocellulosic biomass (Chen et al., 2012; Haykiri-Acma and Yaman, 2010; Kar, 2011; Onay et al., 2007; Park et al., 2010; Vamvuka and Sfakiotakis, 2011; Wu et al., 2014). However, the mechanisms on the synergistic effect were still not very clear. Potential explanations through previous literature focused on the deceleration of repolymerization and cross linking reaction by hydrogen radicals and acceleration of demethoxylation reactions via inorganic matter in lignocellulosic biomass (Soncini et al., 2013; Wu et al., 2014; Yangali et al., 2014). Matsuoka et al. (Matsuoka et al., 2014) proposed that the hydrogen radicals were generated through depolymerization and dehydration during pyrolytic reaction of CE. Those radicals from CE promoted the formation of volatile instead of char during co-pyrolysis process. During LIG pyrolysis process, the reforming of aromatic hydrocarbon structures released hydrogen radicals that can decelerate repolymerization of coal. Furthermore, the formation of LIG char accompanying with softening, melting and fusing (Guo et al., 2014). With the mass ratio of LIG increasing, the melting and fusing of the LIG may block the pore of BC and the gap between BC and LIG. Thus the releasing of volatile may be hampered, negative synergistic effect on the char yields was observed. Previous research on the pyrolysis of lignocellulosic

biomass showed that this process can be mainly divided into three steps without considering the moisture evolution: cellulose decomposition, hemicellulose decomposition and lignin decomposition (Xu and Chen, 2013). A majority of lignocellulosic biomass such as rice straw (Yuan et al., 2012), switch grass (Weiland et al., 2012), hazelnut shell (Haykiri-Acma and Yaman, 2010), corn and sugarcane residues (Aboyade et al., 2013) pine sawdust (Soncini et al., 2013) and pine chips (Pan et al., 1996) mainly consist of cellulose, hemicellulose, lignin. During the co-pyrolysis process of coal and lignocellulosic biomass, the three main compounds may compete against each other on the char generation. In other words, the competition of positive and negative effect from the three model compounds may be the reason for the conflicting reports on the existing of synergistic effect (Pottmaier et al., 2013; Zhang et al., 2011).

### 3.3. Kinetic analysis

Results of the isoconversional method analysis for raw samples and their blends are presented in Tables 3–5, including the values of activation energy ($E$) together with the correlation coefficients. The correlation coefficients ($R^2$) of the $E$ calculated under selected value of $\alpha$ ($0.20 \leqslant \alpha \leqslant 0.80$) were within a narrow range, which indicated that the data was fitted with satisfactory. As can be seen from Table 3, the $E$ of BC decreased with increasing $\alpha$, which was consistent with previous research. The changes of $E$ for CE were not obvious with $\alpha$, from 126.19–146.40 kJ mol$^{-1}$. Previous research on $E$ distribution of CE thermal decomposition were in the range of 120–240 kJ mol$^{-1}$ (Cai et al., 2013; Sanchez-Silva et al., 2012). These values were agreement well with the experimental results in Table 3. The average $E$ values for HCE and LIG were 117.67 kJ mol$^{-1}$and 184.50 kJ mol$^{-1}$.

Distribution on $E$ values for BC blends with lignocellulosic biomass model components are presented in Fig. 6. As can be seen from Fig. 6a, the $E$ values of CE and BCCE mixtures were lower than those of BC under all the selected value of $\alpha$ ($0.20 \leqslant \alpha \leqslant 0.80$). The average $E$ values of BC and CE mixtures were 129.03 kJ mol$^{-1}$, 113.13 kJ mol$^{-1}$ and 122.98 kJ mol$^{-1}$ for BCCE3-1, BCCE1-1 and BCCE1-3. The addition of CE to BC decreased the average $E$ values, from 271.35 kJ mol$^{-1}$ to 122.98 kJ mol$^{-1}$. Furthermore, in Section 3.2, the synergistic effect during co-pyrolysis of BC and CE were more visible for BCCE1-1. This fact suggested that 50% of CE may be an optimal mass ratio for adding to the BC during co-pyrolysis.

The average $E$ value for BCHCE decreased to a minimum value at 105.23 kJ mol$^{-1}$ (BCHCE1-1) then increased with the increase of HCE mass ratio at 246.96 kJ mol$^{-1}$, which was higher than that of HCE. It can be observed from Fig. 6b that just the $E$ values of HCE and BCHCE1-1 were lower than those of BC under all the selected value of $\alpha$. Whit the $\alpha$ raised, the $E$ value of BCHCE1-3 and BCHCE3-1 approached and beyond that of BC. These were consistent with

**Table 3**
Kinetics parameters of the BC and CE calculated by FWO method.

| $\alpha$ | BC | | BCCE3-1 | | BCCE1-1 | | BCCE1-3 | | CE | |
|---|---|---|---|---|---|---|---|---|---|---|
| | $E$ (kJ mol$^{-1}$) | $R^2$ | $E$ (kJ mol$^{-1}$) | $R^2$ | $E$ (kJ mol$^{-1}$) | $R^2$ | $E$ (kJ mol$^{-1}$) | $R^2$ | $E$ (kJ mol$^{-1}$) | $R^2$ |
| 0.2 | 378.18 | 0.9138 | 139.95 | 0.9588 | 130.26 | 0.9328 | 136.31 | 0.9983 | 146.40 | 0.9520 |
| 0.3 | 338.24 | 0.9488 | 130.58 | 0.9798 | 122.25 | 0.9059 | 130.48 | 0.9948 | 136.02 | 0.9955 |
| 0.4 | 264.77 | 0.9990 | 117.40 | 0.9819 | 113.46 | 0.9253 | 121.93 | 0.9936 | 134.06 | 0.9814 |
| 0.5 | 266.03 | 0.9806 | 111.59 | 0.9632 | 116.63 | 0.9126 | 120.92 | 0.9962 | 128.88 | 0.9771 |
| 0.6 | 251.25 | 0.9314 | 128.34 | 0.9999 | 112.01 | 0.9056 | 113.20 | 0.9904 | 127.55 | 0.9990 |
| 0.7 | 176.00 | 0.9533 | 136.62 | 0.9815 | 112.85 | 0.9431 | 112.67 | 0.9935 | 126.19 | 0.9978 |
| 0.8 | 224.91 | 0.9712 | 138.70 | 0.9838 | 84.45 | 0.9126 | 125.33 | 0.9890 | 142.79 | 0.9956 |
| Average | 271.35 | – | 129.03 | – | 113.13 | – | 122.98 | – | 134.56 | – |

**Table 4**
Kinetics parameters of the BC and HCE calculated by FWO method.

| $\alpha$ | BC | | BCHCE3-1 | | BCHCE1-1 | | BCHCE1-3 | | HCE | |
|---|---|---|---|---|---|---|---|---|---|---|
| | $E$ (kJ mol$^{-1}$) | $R^2$ | $E$ (kJ mol$^{-1}$) | $R^2$ | $E$ (kJ mol$^{-1}$) | $R^2$ | $E$ (kJ mol$^{-1}$) | $R^2$ | $E$ (kJ mol$^{-1}$) | $R^2$ |
| 0.2 | 378.18 | 0.9138 | 177.30 | 0.9946 | 84.65 | 0.9213 | 266.05 | 0.9966 | 93.62 | 0.9824 |
| 0.3 | 338.24 | 0.9488 | 174.99 | 0.9948 | 91.89 | 0.9029 | 263.67 | 0.9896 | 120.27 | 0.9561 |
| 0.4 | 264.77 | 0.9990 | 212.43 | 0.9750 | 113.30 | 0.9189 | 310.45 | 0.9773 | 129.29 | 0.9763 |
| 0.5 | 266.03 | 0.9806 | 228.14 | 0.9672 | 116.82 | 0.9604 | 278.74 | 0.9841 | 142.76 | 0.9938 |
| 0.6 | 251.25 | 0.9314 | 248.72 | 0.9938 | 100.69 | 0.9979 | 273.82 | 0.9943 | 146.74 | 0.9723 |
| 0.7 | 176.00 | 0.9533 | 225.45 | 0.9718 | 113.87 | 0.9982 | 134.73 | 0.8792 | 86.78 | 0.9981 |
| 0.8 | 224.91 | 0.9712 | 193.18 | 0.9990 | 115.40 | 0.9912 | 201.23 | 0.9580 | 104.25 | 0.9961 |
| Average | 271.35 | – | 208.60 | – | 105.23 | – | 246.96 | – | 117.67 | – |

**Table 5**
Kinetics parameters of the BC and LIG calculated by FWO method.

| $\alpha$ | BC | | BCLIG3–1 | | BCLIG1–1 | | BCLIG1–3 | | LIG | |
|---|---|---|---|---|---|---|---|---|---|---|
| | $E$ (kJ mol$^{-1}$) | $R^2$ | $E$ (kJ mol$^{-1}$) | $R^2$ | $E$ (kJ mol$^{-1}$) | $R^2$ | $E$ (kJ mol$^{-1}$) | $R^2$ | $E$ (kJ mol$^{-1}$) | $R^2$ |
| 0.2 | 378.18 | 0.9138 | 153.12 | 0.9519 | 83.55 | 0.9686 | 122.75 | 0.9924 | 322.30 | 0.9336 |
| 0.3 | 338.24 | 0.9488 | 205.53 | 0.8842 | 125.76 | 0.8994 | 135.14 | 0.9974 | 295.34 | 0.9716 |
| 0.4 | 264.77 | 0.9990 | 293.52 | 0.9093 | 125.33 | 0.9011 | 168.42 | 0.9998 | 220.48 | 0.9463 |
| 0.5 | 266.03 | 0.9806 | 427.46 | 0.9981 | 129.93 | 0.9879 | 276.26 | 0.9667 | 261.34 | 0.9752 |
| 0.6 | 251.25 | 0.9314 | 391.06 | 0.9343 | 161.96 | 0.9431 | 316.60 | 0.9999 | 161.56 | 0.9933 |
| 0.7 | 176.00 | 0.9533 | 383.70 | 0.9876 | 209.08 | 0.9751 | 346.33 | 0.9929 | 144.50 | 0.9882 |
| 0.8 | 224.91 | 0.9712 | 450.05 | 0.9740 | 255.51 | 0.9981 | 212.08 | 0.8814 | 109.74 | 0.9866 |
| Average | 271.35 | – | 329.21 | – | 155.87 | – | 225.37 | – | 184.50 | – |

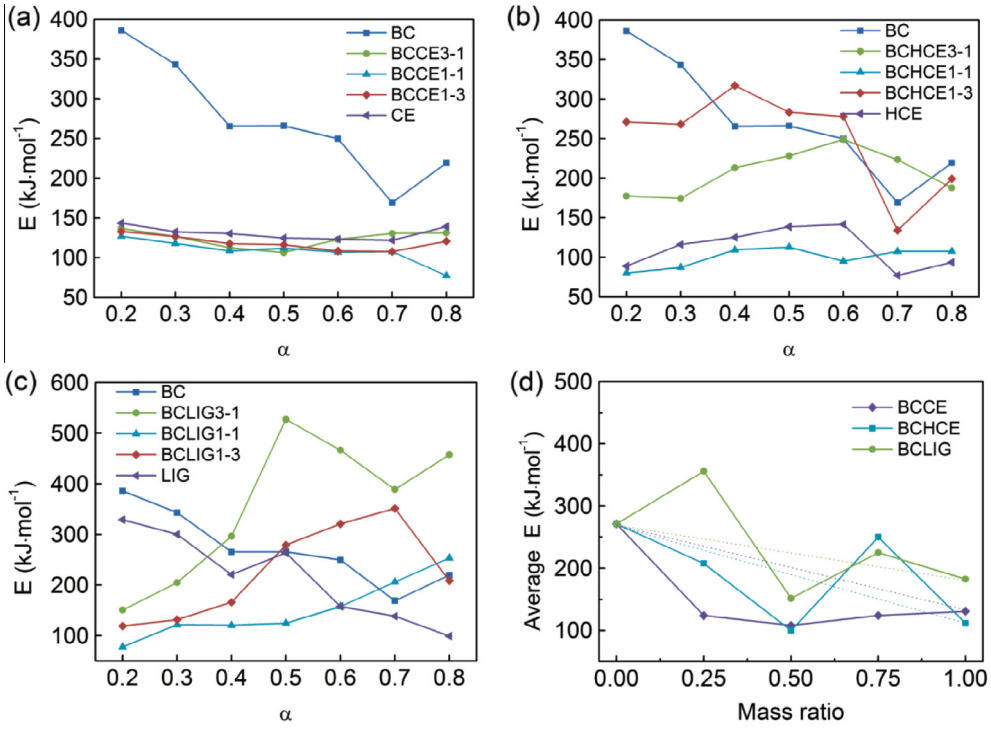


**Fig. 6.** Distribution and average values of the activation energy for BC blends with lignocellulosic biomass model components, (a) BC blends with CE, (b) BC blends with HCE, (c) BC blends with LIG, (d) average values of the activation energy (dotted lines were the predicted value of the average *E* based on the weighted average of the BC and model compounds).

the synergistic effect during co-pyrolysis of BC and HCE. The diminution of the *E* values was in favor of the thermal decomposition of the samples. Compared with BCHCE3-1 and BCHCE1-3, BCHCE 1-1 showed minimal influence on the passive synergistic effect from Fig. 5d. Thus, 50% of HCE may be beneficial to reduce the passive synergistic effect to minimum.

As shown in Fig. 6c, the values of *E* for LIG decreased with the increment of $\alpha$, which was similar to that of BC. However, the tendency for *E* values of BCLIG3-1 firstly reached the maximum under $\alpha = 0.5$ and then deceased. While for BCLIG1-1 and BCLIG 1-3, the value of *E* generally increased with the co-pyrolysis process proceed. The variation tendency for average *E* values of BC blended with lignocellulosic biomass model components is presented in Fig. 6d. The dotted lines were the predicted value of the average *E* based on the weighted average of the BC and model compounds. The average *E* values of the BCCE mixtures and BCHCE mixtures pyrolysis were less than the predicted value which can be calculated by weighed average method according to the *E* values of individual samples and mass ratio except the BCHCE1-3. The observed nonadditivity performance of the average *E* values indicated that the synergistic effects existed during co-pyrolysis of BC and model compounds.

Previous research suggested that the variation of *E* during pyrolysis of carbonous materials involved marked changes in solid structure (Sonoyama and Hayashi, 2013; Yangali et al., 2014). The pyrolysis of CE had a tendency to amorphous solid or softening through cyclic aliphatic units transformed to aromatic structures with decreasing of *E*. During the co-pyrolysis of CE and BC, the formation of amorphous structure and aromatisation of CE may exert significant effect on the formation of co-pyrolysis char. Thus the lower *E* value of the mixtures would be explained by the marked solid structure changes of CE and BC. The increasing *E* value of BCHCE and BCLIG mixtures with $\alpha$ was indicated with co-pyrolysis char forming by carbonisation.

Although the above findings (non-additive char production and non-additivity performance of the average *E*) provided a reasonably basis for proving that the synergistic effects existed during the co-pyrolysis process, additional studies should be provided further information on the mechanism of these effects. In particular, analysis on the structure evolution of the co-pyrolysis char may indicate the effect of different kind and mass ratio of the model compounds on the char yields. Moreover, the transformation of the gas and tar products could give a sense for the synergistic effects on the product distributions.

## 4. Conclusion

Positive synergy effect of cellulose to generate less char during co-pyrolysis was pronounced above 360 °C. Positive or negative synergistic of hemicellulose and lignin on char yields were depended upon the mixed ratio and temperature range. Nonadditivity performance of the activation energy values of the coal and three model compounds blends was also observed. These variations of activation energy were related to the solid structure changed of the co-pyrolysis char. This work suggested that the synergistic effects on thermal behavior during co-pyrolysis of lignocellulosic biomass and coal would be caused by the competition effects of the three model compounds.

## Acknowledgements

This work was financially supported by the Low-carbon Development Special Fund of Guangdong Province, China. The authors are thankful Zhihui Wu, Caijian Zeng from GuangDong Xi'an Jiaotong University Academy for their support of this work. Z.Q.W. is also grateful to Dongxia Ouyang from Zhong Tai Creative Holdings for her valuable suggestions.

## References


Aboyade, A.O., Görgens, J.F., Carrier, M., Meyer, E.L., Knoetze, J.H., 2013. Thermogravimetric study of the pyrolysis characteristics and kinetics of coal blends with corn and sugarcane residues. Fuel Process. Technol. 106, 310–320.

Cai, J.M., Wu, W.X., Liu, R.H., 2013. Sensitivity analysis of three-parallel-DAEM-reaction model for describing rice straw pyrolysis. Bioresour. Technol. 132, 423–426.

Chen, C., Ma, X., He, Y., 2012. Co-pyrolysis characteristics of microalgae *Chlorella vulgaris* and coal through TGA. Bioresour. Technol. 117, 264–273.

Dumitriu, S., 2012. Polysaccharides: Structural Diversity and Functional Versatility, second ed. Taylor & Francis.

Guo, D.L., Yuan, H.Y., Yin, X.L., Wu, C.Z., Wu, S.B., Zhou, Z.Q., 2014. Effects of chemical form of sodium on the product characteristics of alkali lignin pyrolysis. Bioresour. Technol. 152, 147–153.

Habibi, R., Kopyscinski, J., Masnadi, M.S., Lam, J., Grace, J.R., Mims, C.A., Hill, J.M., 2013. Co-gasification of biomass and non-biomass feedstocks: synergistic and inhibition effects of switchgrass mixed with sub-bituminous coal and fluid coke during $CO_2$ gasification. Energy Fuels 27 (1), 494–500.

Haykiri-Acma, H., Yaman, S., 2010. Interaction between biomass and different rank coals during co-pyrolysis. Renewable Energy 35 (1), 288–292.

Jianguo, X., Zhaolong, W., 1999. The study of pyrolysis property of pulverized coal by thermogravimetry. J. Combust. Sci. Technol. 5 (2), 175–179.

Kar, Y., 2011. Co-pyrolysis of walnut shell and tar sand in a fixed-bed reactor. Bioresour. Technol. 102 (20), 9800–9805.

Kissinger, H.E., 1957. Reaction kinetics in differential thermal analysis. Anal. Chem. 29 (11), 1702–1706.

Lopez-Gonzalez, D., Fernandez-Lopez, M., Valverde, J.L., Sanchez-Silva, L., 2013. Thermogravimetric-mass spectrometric analysis on combustion of lignocellulosic biomass. Bioresour. Technol. 143, 562–574.

Maschio, G., Koufopanos, C., Lucchesi, A., 1992. Pyrolysis, a promising route for biomass utilization. Bioresour. Technol. 42 (3), 219–231.

Matsuoka, S., Kawamoto, H., Saka, S., 2014. What is active cellulose in pyrolysis? An approach based on reactivity of cellulose reducing end. J. Anal. Appl. Pyrol. 106, 138–146.

Moghtaderi, B., Meesri, C., Wall, T.F., 2004. Pyrolytic characteristics of blended coal and woody biomass. Fuel 83 (6), 745–750.

Onay, Ö., Bayram, E., Koçkar, Ö.M., 2007. Copyrolysis of seyitömer–lignite and safflower seed: influence of the blending ratio and pyrolysis temperature on product yields and oil characterization. Energy Fuels 21 (5), 3049–3056.

Pan, Y.G., Velo, E., Puigjaner, L., 1996. Pyrolysis of blends of biomass with poor coals. Fuel 75 (4), 412–418.

Park, D.K., Kim, S.D., Lee, S.H., Lee, J.G., 2010. Co-pyrolysis characteristics of sawdust and coal blend in TGA and a fixed bed reactor. Bioresour. Technol. 101 (15), 6151–6156.

Parshetti, G.K., Hoekman, S.K., Balasubramanian, R., 2013. Chemical, structural and combustion characteristics of carbonaceous products obtained by hydrothermal carbonization of palm empty fruit bunches. Bioresour. Technol. 135, 683–689.

Pottmaier, D., Costa, M., Farrow, T., Oliveira, A.A.M., Alarcon, O., Snape, C., 2013. Comparison of rice husk and wheat straw: from slow and fast pyrolysis to char combustion. Energy Fuels 27 (11), 7115–7125.

Richards, G.N., 1987. Glycolaldehyde from pyrolysis of cellulose. J. Anal. Appl. Pyrol. 10 (3), 251–255.

Sadhukhan, A.K., Gupta, P., Goyal, T., Saha, R.K., 2008. Modelling of pyrolysis of coal–biomass blends using thermogravimetric analysis. Bioresour. Technol. 99 (17), 8022–8026.

Sanchez-Silva, L., Lopez-Gonzalez, D., Villasenor, J., Sanchez, P., Valverde, J.L., 2012. Thermogravimetric-mass spectrometric analysis of lignocellulosic and marine biomass pyrolysis. Bioresour. Technol. 109, 163–172.

Shen, D.K., Gu, S., Bridgwater, A.V., 2010. The thermal performance of the polysaccharides extracted from hardwood: cellulose and hemicellulose. Carbohydr. Polym. 82 (1), 39–45.

Soncini, R.M., Means, N.C., Weiland, N.T., 2013. Co-pyrolysis of low rank coals and biomass: product distributions. Fuel 112, 74–82.

Sonoyama, N., Hayashi, J., 2013. Characterisation of coal and biomass based on kinetic parameter distributions for pyrolysis. Fuel 114, 206–215.

Vamvuka, D., Sfakiotakis, S., 2011. Combustion behaviour of biomass fuels and their blends with lignite. Thermochim. Acta 526 (1–2), 192–199.

Wang, L.L., Guo, Y.P., Zhu, Y.C., Qu, Y.N., Li, Y., Rong, C.G., Wang, Z.C., Liu, Y.H., 2011. Investigation on catalyzed combustion of wheat straw by thermal analysis. Thermochim. Acta 512 (1–2), 254–257.

Weiland, N.T., Means, N.C., Morreale, B.D., 2012. Product distributions from isothermal co-pyrolysis of coal and biomass. Fuel 94 (1), 563–570.

Wu, Z.Q., Wang, S.Z., Zhao, J., Chen, L., Meng, H.Y., 2014. Thermal behavior and char structure evolution of bituminous coal blends with edible fungi residue during co-pyrolysis. Energy Fuels 28 (3), 1792–1801.

Xu, Y.L., Chen, B.L., 2013. Investigation of thermodynamic parameters in the pyrolysis conversion of biomass and manure to biochars using thermogravimetric analysis. Bioresour. Technol. 146, 485–493.

Yan, W.P., Chen, Y.Y., 2007. Interaction performance of co-pyrolysis of biomass mixture and coal of different rank. Proc. CSEE 27 (2), 80–86.

Yangali, P., Celaya, A.M., Goldfarb, J.L., 2014. Co-pyrolysis reaction rates and activation energies of West Virginia coal and cherry pit blends. J. Anal. Appl. Pyrolysis. (in press).

Yuan, S., Dai, Z.H., Zhou, Z.J., Chen, X.L., Yu, G.S., Wang, F.C., 2012. Rapid co-pyrolysis of rice straw and a bituminous coal in a high-frequency furnace and gasification of the residual char. Bioresour. Technol. 109, 188–197.

Zhang, X.L., Yang, W.H., Blasiak, W., 2011. Modeling study of woody biomass: interactions of cellulose, hemicellulose, and lignin. Energy Fuels 25 (10), 4786–4795.